A Muscle Synergy-Inspired Method of Detecting Human Movement Intentions Based on Wearable Sensor Fusion

Yi-Xing Liu, Ruoli Wang, and Elena M. Gutierrez-Farewik

***Abstract*— Detecting human movement intentions is fundamental to neural control of robotic exoskeletons, as it is essential for achieving seamless transitions between different locomotion modes. In this study, we enhanced a muscle synergy-inspired method of locomotion mode identification by fusing the electromyography data with two types of data from wearable sensors (inertial measurement units), namely linear acceleration and angular velocity. From the finite state machine perspective, the enhanced method was used to systematically identify 2 static modes, 7 dynamic modes, and 27 transitions among them. In addition to the five broadly studied modes (level ground walking, ramps ascent/descent, stairs ascent/descent), we identified the transition between different walking speeds and modes of ramp walking at different inclination angles. Seven combinations of sensor fusion were conducted, on experimental data from 8 able-bodied adult subjects, and their classification accuracy and prediction time were compared. Prediction based on a fusion of electromyography and gyroscope (angular velocity) data predicted transitions earlier and with higher accuracy. All transitions and modes were identified with a total average classification accuracy of 94.5% with fused sensor data. For nearly all transitions, we were able to predict the next locomotion mode 300-500 ms prior to the step into that mode.**

***Index Terms*— Intent recognition, locomotion modes identification, muscle synergies, sensor fusion, robotic exoskeletons.**

I. Introduction

ROBOTIC exoskeletons have extended their movement assistance focus from only level-ground walking to include various locomotion modes, such as ramp walking and stair ascent/descent. To efficiently assist multiple locomotion modes, powered exoskeletons should transition between different locomotion modes seamlessly. A few commercially-available exoskeletons adjust their assistance strategies between different modes using signals from remote controls, non-intuitive muscle contractions, and physical signals such as tapping the foot [1], [2], none of which provide seamless transitions between different locomotion modes.

Achieving seamless transitions between locomotion modes requires accurate movement intention detection. To this end, both model-based approaches, i.e. using neural driven musculoskeletal models [3], and model-free approaches, i.e. machine learning algorithms including Mahalanobis distance, support vector machine, linear discriminant analysis, and artificial neural networks [4]–[7], have been implemented to identify locomotion modes and the transitions between them. Sartori *et al.* [8] proposed a standalone knee joint model using an EMG-driven musculoskeletal model to accurately estimate joint moments of dynamic movements for assistive devices. Huang *et al.* [9] presented a real-time implementation for locomotion modes identification using a support vector machine with electromyography (EMG) signals and mechanical sensors (6-DOF load cells) from a prosthetic knee. In their method, the gait cycle was divided into three stance sub-phases and a swing phase. A separate classifier was trained for each phase, and a decision was voted by the four classifiers through a majority voting method. Young *et al.* [5] presented a similar study aim, but used dynamic Bayesian networks to integrate time series information, and demonstrated that the signal analysis window at either heel strike or toe-off performed better than the multiple analysis windows. Afzal *et al.* [10] developed a new method for locomotion mode identification using muscle synergies from EMG signals. They first extracted three time-domain features (root mean square, waveform length, and maximum value) from each EMG signal to construct the feature matrices. They reduced the dimensions of the feature matrices using the non-negative matrix factorization (NMF) algorithm, then reconstructed them using the non-negative least square (NNLS) algorithm. Classification was made based on finding the highest similarity between the reconstructed feature matrix and the original feature matrix, and was reported as more accurate than support vector machine, linear discriminant analysis, and artificial neural networks methods. However, their presented muscle synergy method for locomotion mode

Manuscript received November 11, 2020; revised March 19, 2021 and April 15, 2021; accepted June 2, 2021. Date of publication June 7, 2021; date of current version June 15, 2021. The project was generously funded by the Promobilia Foundation (ref nr 18200) and the Swedish Research Council (ref 2018-00750 BADASS: BiomechAnics in motion Disorders and ASSistance). *(Corresponding author: Elena M. Gutierrez-Farewik.)*

This work involved human subjects or animals in its research. Approval of all ethical and experimental procedures and protocols was granted by the Local Ethical Board, Stockholm, Sweden, under Approval No. Dnr. 2020-02311.

Yi-Xing Liu is with the KTH MoveAbility Lab, Department of Engineering Mechanics, KTH Royal Institute of Technology, 10044 Stockholm, Sweden, and also with the KTH BioMEx Center, KTH Royal Institute of Technology, 10044 Stockholm, Sweden.

Ruoli Wang and Elena M. Gutierrez-Farewik are with the KTH MoveAbility Lab, Department of Engineering Mechanics, KTH Royal Institute of Technology, 10044 Stockholm, Sweden, also with the KTH BioMEx Center, KTH Royal Institute of Technology, 10044 Stockholm, Sweden, and also with the Department of Women's and Children's Health, Karolinska Institutet, 17177 Stockholm, Sweden (e-mail: lanie@kth.se).

Digital Object Identifier 10.1109/TNSRE.2021.3087135

identification had a relatively high classification error in identifying certain transitions, namely when muscle synergy patterns were too similar to differentiate. Other studies have likewise reported that muscle synergy patterns in different walking speeds and in running are similar to that in level ground walking [11]–[14]. As such, muscle synergy methods based only on EMG signals have limited potential in distinguishing several locomotion modes.

Sensor types influence an algorithm's classification performance to a great extent. EMG signals can be particularly useful in detecting movement intentions, as the activation they detect precedes muscle-tendon length changes and thus movements. Huang *et al.* [9] reported more accurate predictions of movement intention when EMG signals were fused with mechanical sensor data vs. predicting from only the mechanical sensor data. Furthermore, EMG are broadly used in human-machine interfaces for exoskeletons, i.e. using EMG-driven neuromusculoskeletal model to estimate joint torques [3]. However, EMG signals are complicated and sensitive to electrode placement and to disturbances such as soft tissue artifact, cross-talk, and pressure [15]. A classifier based solely on EMG signals is thus vulnerable to such disturbances and is of limited use on persons with muscle weakness and/or disorders affecting muscle tone. To this end, combining EMG sensors with mechanical sensors has become a more and more common approach for achieving high classification performance [16]–[20]. Several studies describe methods to identify locomotion modes and transitions among them based on integrating EMG signals with ground reaction forces [21], accelerometers [22], [23], and both accelerometers and gyroscopes [24]. Tanghe *et al.* [25] fused different types of mechanical sensors to predict gait events and joint trajectories through a probabilistic principle component model. Results from these studies indicate that sensor fusion methods can increase the accuracy and robustness of a myoelectrical control system.

Several studies on locomotion mode identification report investigations of 5 different modes, namely level ground walking, stairs ascent, stairs descent, ramp ascent and ramp descent, as well as the 8 transitions among them [2], [26]–[28], that is, from level ground walking to ramp/stairs ascent/descent, and from ramp/stairs ascent/descent to level ground walking. A few studies have also investigated stepping over an obstacle [9], turning in different directions [7], sit-to-stand and stand-to-sit tasks [26], [29]. Sup *et al.* [30] studied walking on two different inclination angles (5° and 10°), using a ground slope estimator to identify the incline walking mode. However, no study has systematically evaluated all the above movements and the transitions among them, such as from quiet standing to level ground walking and from walking to stop. Even if a classifier can distinguish five locomotion modes with a high classification accuracy, its performance may not be reliable in a classification problem with more than 5 locomotion modes. A greater number of movements and locomotion modes should be studied to improve the robustness of classification algorithms.

In this study, we aim to investigate whether classification accuracy of a muscle synergy-inspired method in locomotion mode identification can be improved by fusing EMG signals with signals from mechanical sensors. We furthermore aim to classify among static and dynamic modes as well as the transitions between them, with a focus on predicting each transition and on the prediction time required for identifying each transition.

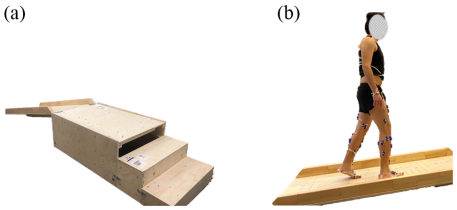

Fig. 1. (a) The ramp-stairs module; (b) One subject, equipped with EMG and IMU sensors, walking on the module. The subject provided written consent for use of this image.

II. Methods

A. Participants

Eight subjects without any musculoskeletal disorders or recent lower-extremity injuries (4F/4M, height: 171.4 ± 9.3 cm, weight: 62.3 ± 12.65 kg, age: 28.25 ± 1.39 years) were recruited to take part in the experiments. The experiments were approved by the local ethical board, Stockholm, Sweden (Dnr. 2020-02311). All subjects provided written consent. Participation was voluntary and could be terminated at any time.

B. Experimental Protocol and Data Collection

Experiments were conducted in the KTH MoveAbility lab, equipped with a 10-camera motion capture system (Vicon V16), 3 force plates (AMTI), wireless EMG (Myon aktos) sensors, and inertial measurement units (IMU) sensors (Myon aktos-t). Surface EMG data was recorded on eleven muscles on the right limb – rectus femoris, vastus medialis, vastus lateralis, tibialis anterior, medialis and lateralis gastocnemius, soleus, gluteus maximus, gluteus mediums, peroneus longus, and semitendious – and nine muscles on the left limb – rectus femoris, vastus medialis, vastus lateralis, tibialis anterior, medialis gastrocnemius, soleus, gluteus mediums, peroneus longus, and semitendious. EMG electrodes were placed according to SENIAM recommendations [31]. Seven IMU sensors were placed on the left and right thighs, shanks, and feet, and one on the waist (Fig. 1). Foot switches were placed under the toe and heel of each foot, and were used to detect heel-strike and toe-off events. All experimental data were sampled at 2000 Hz.

A tailored ramp-stairs module with three adjustable inclination angles (4°(A_1), 8°(A_2), 12°(A_3)) and stairs with 18 cm rise and 28 cm run was used in the measurement (Fig. 1(a)). For each inclination angle, subjects started from standing still, then walked on the module in two directions, i.e. ramps-to-stairs, in which the first ascended a ramp, traversed a small platform then walked down 1 to 3 steps, or stairs-to-ramp, the opposite as previous. In the ramp-to-stairs direction, there were 15 step-to-step types: standing still to level ground walking (ST→W), level ground walking to level ground walking (W→W), level ground walking to ramp ascending (W→RA_1,W→RA_2, and W→RA_3), ramp ascending to ramp ascending (RA_1→RA_1, RA_2→RA_2,

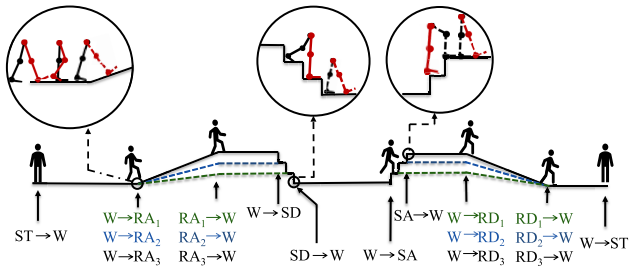

Fig. 2. Transitions involved in the dynamic states. The limb in focus is shown in red. Solid lines indicate the limb positions prior to the transition, and dashed lines indicate the limb positions during the first step in the next mode. ST: standing still, W: level ground walking, RA: ramp ascent, SD: stairs descent, SA: stairs ascent, and RD: ramp descent. Subscripts 1-3 indicate different angles of ramp ascent/descent.

and $RA_3 \rightarrow RA_3$), ramp ascending to level ground walking ($RA_1 \rightarrow W$, $RA_2 \rightarrow W$, and $RA_3 \rightarrow W$), level ground walking to stair descending ($W \rightarrow SD$), stair descending to stair descending ($SD \rightarrow SD$), stair descending to level ground walking ($SD \rightarrow W$), and level ground walking to standing still ($W \rightarrow ST$). In the stairs-to-ramp direction, besides some of the same modes, there were another 12 transitions, namely level ground walking to stair ascending ($W \rightarrow SA$), stair ascending to stair ascending ($SA \rightarrow SA$), stair ascending to level ground walking ($SA \rightarrow W$), level ground walking to ramp descending ($W \rightarrow RD_1$,$W \rightarrow RD_2$, and $W \rightarrow RD_3$), ramp descending to ramp descending ($RD_1 \rightarrow RD_1$, $RD_2 \rightarrow RD_2$, and $RD_3 \rightarrow RD_3$), and ramp descending to level ground walking ($RD_1 \rightarrow W$, $RD_2 \rightarrow W$, and $RD_3 \rightarrow W$, Fig. 2). For transitions involving stairs, subjects ascended or descended one step in transitions $W \rightarrow SA/SD$ and $SA/SD \rightarrow W$, and two steps in transitions $SA \rightarrow SA$ and $SD \rightarrow SD$. In addition, each subject performed several more motions: sit-to-stand ($Sit \rightarrow ST$), stand-to-sit ($ST \rightarrow Sit$), walking to stepping over an obstacle ($W \rightarrow O$), and changing walking speed from normal speed to a fast speed ($W \rightarrow FW$). While some of these 27 step-to-step types are transitions between locomotion modes and others are simply another step in the same mode, in the interest of clarity, they are be referred to as "transitions" from this point forward. Each task was repeated for at least 10 trials. During the whole session, all the subjects were encouraged to walk at a self-selected, comfortable speed and to try to maintain this speed as closely as possible.

C. Enhanced Muscle Synergy Inspired Method

The enhanced algorithm was designed based on the algorithm developed by Afzal *et al.* [10]. Assuming that we have a training data set with P different transitions, for each transition's training data, the non-negative matrix factorization (NMF) algorithm was used to reduce the dimensions of the feature matrix F^i_{train}.

$$W_i, C = \text{NMF}(F^i_{\text{train}}), \quad i = 1, 2, \ldots, P \tag{1}$$

where, W_i is the extracted weight matrix that describes the linear relationship between each feature in the original feature matrix and each component in the reduced dimension matrix for the i_{th} transition, and C is the extracted action signals for each component in the reduced dimension matrix, namely the command vector.

For each feature matrix of the test data f_{test}, a non-negative least squares (NNLS) algorithm was used to estimate the command vector c^i_{test} with W_i and f_{test} (2). Then, feature vectors $\hat{f}^i_{\text{test}}$ for each test data were reconstructed by multiplying the command vector c^i_{test} with the weight matrix W_i (3). Finally, classification results were made by computing the cosine similarity S^i_{test} between the reconstructed feature vector $\hat{f}^i_{\text{test}}$ and the actual feature vector f_{test}. The predicted mode was the mode with the maximum similarity (Fig. 3).

$$c^i_{\text{test}} = \text{NNLS}(W_i, f_{\text{test}}), \quad i = 1, 2, \ldots, P \tag{2}$$

$$\hat{f}^i_{\text{test}} = W_i \times c^i_{\text{test}}, \quad i = 1, 2, \ldots, P \tag{3}$$

We enhanced this algorithm at the feature extraction step. Instead of only using EMG data, we fused EMG data with IMU sensor data, namely linear acceleration (Acc) from accelerometers and angular velocity from gyroscopes (Gyr). Raw EMG and raw IMU data (Acc and Gyr) were used to extract features. Six time-domain features were extracted from Acc and Gyr data: mean absolute value, zero crossing variance, root mean square, slope sign changes and wave length. Four time-domain features were extracted from EMG data: mean absolute value, zero crossing, variance, wave length [22]. In each sensor-fused configuration, features of the selected sensors were concatenated into one feature matrix for each analysis window. The algorithm was implemented with Python. The NMF and the NNLS algorithms used in our study were from Scikit-learn and SciPy respectively.

D. System Design

We adopted the concept of finite state machine to design the classification system [32], [33]. Instead of training one classifier to identify all transitions, we trained 6 classifiers, namely the static state, the walking state, the ramp ascent state (RA), the ramp descent state (RD), and the stairs ascent (SA) state and the descent state (SD) (Fig. 4). The static state classifier was designed to predict intentions from one of two static modes: standing (ST) or sitting (Sit) to either the other static mode or to a walking (W) mode. The transitions identified from the static state are $ST \rightarrow W$, $ST \rightarrow Sit$ and $Sit \rightarrow ST$. If for instance, a $ST \rightarrow W$ was detected, then the system state shifted from a static state to a walking state.

The walking state classifier was designed to identify transitions from walking to the same or another walking mode, namely walking to (continued) walking ($W \rightarrow W$), walking to fast walking ($W \rightarrow FW$) and walking to obstacle clearance ($W \rightarrow O$). The walking state classifier was also designed to identify transitions from walking to another state: from walking to one of the three RA modes ($W \rightarrow RA$), from walking to one of the three RD modes ($W \rightarrow RD$), from walking to stair ascent ($W \rightarrow SA$), from walking to stair descent ($W \rightarrow SD$) and from walking to standing ($W \rightarrow ST$). We first performed a preliminary test before designing the classification system, in which we tried to classify the transitions from walking to the three ramp angles individually, i.e. $W \rightarrow RA_{1\text{-}3}$ and $W \rightarrow RD_{1\text{-}3}$. While the classifier could reliably classify

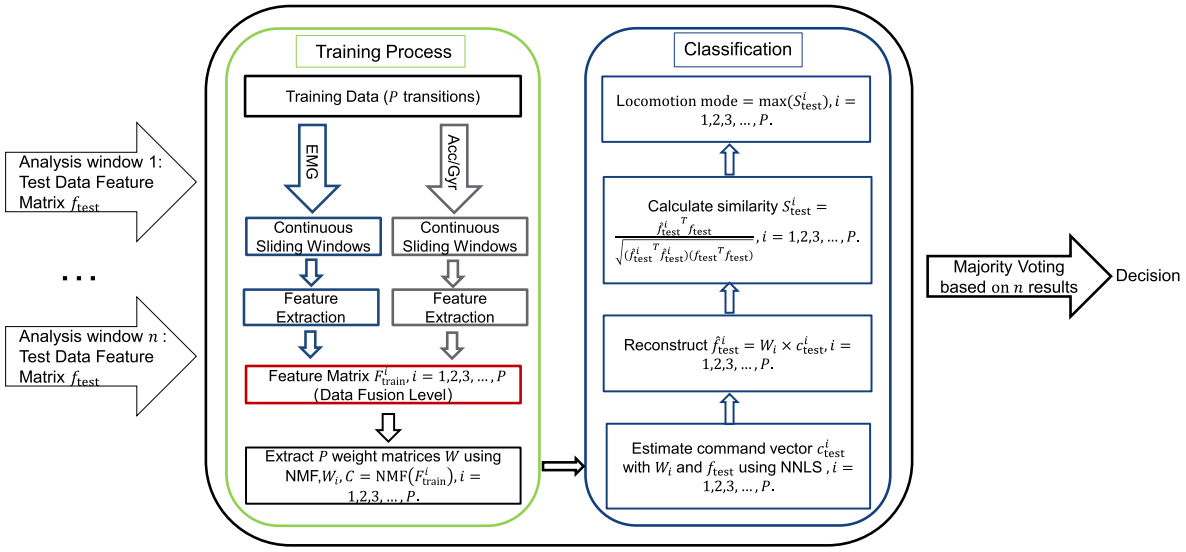

Fig. 3. Process of the enhanced muscle synergy inspired method. The red framed block indicates the enhancement we made to the muscle synergy method, by fusing different kinds of sensor data in the feature extraction level. EMG: electromyography, Acc: accelerometer, Gyr: gyroscope, W_i: the weight matrix for the i_{th} transition, C: the command vector, F^i_{train}: the feature matrix of training data for the i_{th} transition, f_{test}: the original feature matrix of testing data, c^i_{test}: the estimated command vector with W_i and f_{test}, $\hat{f}_{\text{test}}$: the reconstructed feature matrix of testing data, S_{test}: the cosine similarity between the original feature matrix and the reconstruct feature matrix, NMF: the non-negative matrix factorization algorithm, and NNLS: the non-negative least square algorithm.

W→RA and W→RD in general, it was not able to reliably distinguish among W→RA_{1-3}, and among W→RD_{1-3}. Hence, all W→$\text{RA}_{1\text{-}3}$ transitions were grouped into W→RA and all W→$\text{RD}_{1\text{-}3}$ were grouped into W→RD.

The RA state classifier was designed to identify first from each of the three ($\text{RA}_{1\text{-}3}$) modes individually, corresponding to the three ramp angles, to either the same mode or to walking (RA_k→RA_k and RA_k→W, where $k = 1, 2, 3$ refers to the three ramp angles), referred to as the 3-modes classification. It was also designed to identify from any one of the three RA modes to either the same mode or to walking (RA→RA and RA→W), by grouping all ramp angle modes into one RA mode, referred to as the 1-mode classification.

The RD state classifier likewise could identify six transitions from a 3-modes classification (RD_k→RD_k or RD_k→W) where $k = 1, 2, 3$ is the ramp angle, or two transitions from a 1-mode classification (RD→RD or RD→W) wherein the three ramp angles modes are grouped into one RA.

Finally, the stair ascent state classifier was designed to identify the transition to the same state (SA→SA) or to walking (SA→W), and likewise for the stair descent classifier (SD→SD or SD→W).

E. Seven Sensor-Fused Configurations

All dynamic transitions studied were led by the right lower limb, i.e. new mode began at right foot contact (Fig. 2). Thus, data from sensors on the right lower limb are referred to as ipsilateral (Ipsi) and sensor data from both sides is referred to as bilateral (Bi). In each classifier described in Sections II-C and II-D, feature extraction was performed by seven different sensor-fused configurations, namely:

1. Ipsi EMG
2. Bi EMG
3. Ipsi EMG + Bi Acc
4. Ipsi EMG + Bi Gyr
5. Ipsi EMG + Bi Acc + Bi Gyr
6. Bi Acc + Bi Gyr
7. Bi Gyr

While transitions from a static mode were symmetric, the same convention was used and classification was performed based on these same 7 sensor configurations.

F. Analysis Windows and Prediction Time

The classifiers were designed to predict movement intentions, thus, transitions should be detected at or before a critical time point prior to the new step or mode. However, this critical time point is not well-defined. To this end, we defined series of discrete windows preceding the transition to the new mode.

In all dynamic states (W, RA, RD, SA and SD), discrete windows were created throughout the preceding stride, beginning with ipsilateral foot contact, and ending at 100 ms before the ipsilateral foot contact into the next mode. Each window was 200 ms in length, and was slid at 100 ms increments (Fig. 5(a)). The classifier detected the next transition using extracted sensor features from each window. As there were a number of discrete analysis windows during the preceding stride, during which transitions were detected independently of the other windows, the detected transition was determined by a majority vote, based on decisions from all used discrete analysis windows; the transition detected by most analysis windows was regarded as the detected transition. Furthermore, transition detection based on only the earlier analysis windows that occurred during the prior ipsilateral stance phase are referred to as stance phase (St) analysis windows, and transition detection based on analysis windows from both preceding stance and swing phase windows (always excluding

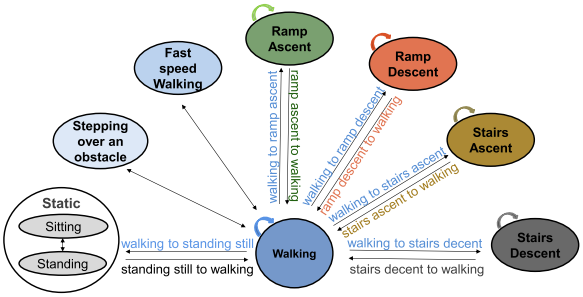

Fig. 4. Illustration of the finite machine states. Eight transitions were detected in the walking state (W): W→W, W→ST (ST: standing), W→O (O: stepping over an obstacle), W→FW (FW: fast speed walking), W→RA (RA: ramp ascent), W→RD (RD: ramp descent), W→SA (SA: stairs ascent), and W→SD (SD: stairs descent). Six transitions were detected in the 3-modes RA classification: $RA_1 \rightarrow RA_1$, $RA_1 \rightarrow W$, $RA_2 \rightarrow RA_2$, $RA_2 \rightarrow W$, $RA_3 \rightarrow RA_3$, and $RA_3 \rightarrow W$, and two transitions were detected when all ramp angles were combined into a 1-mode classification: RA→RA and RA→W. Likewise, six transitions were detected in the 3-modes RD classification:$RD_1 \rightarrow RD_1$, $RD_1 \rightarrow W$, $RD_2 \rightarrow RD_2$, $RD_2 \rightarrow W$, $RD_3 \rightarrow RD_3$, and $RD_3 \rightarrow W$, and two in the 1-mode RD state: RD→RD and RD→W. Two transitions were detected in the SA state: SA→SA and SA→W, and two in the SD state: SD→SD and SD→W. Three transitions were detected in the static state: Sit→ST (Sit: sitting), ST→Sit, and ST→W.

the 100 ms preceding the step into the next mode) are referred to as stance+swing (St+Sw) analysis windows. Classification based on St analysis windows thus occurs earlier than during St+Sw windows.

In static states, the analysis windows of Sit→ST, ST→Sit and ST→W were also 200 ms long, and began 1000 ms prior to lower limb movement initiation (Fig. 5(b-c)), or ipsilateral toe-off in ST→W, and concluded in four variations: 500 ms, 400 ms, 300 ms and 200 ms prior to movement initiation, based again on majority voting. Thus four different lengths of analysis windows were tested for each subjects' static state, corresponding to four possible detection times.

The prediction time was defined as the time when the transition was detected accurately prior to the step into a new mode. For each transition, we analyzed both classification accuracy and analysis time. For St analysis windows, the prediction time was defined as the time instance of the end of the last analysis window prior to ipsilateral foot contact at which the predicted transition was accurate. Similarly for St+Sw analysis windows, at least one Sw analysis was always included, and prediction time was defined similarly. For the transitions involved in the static state, the prediction time was defined as the time instance at end of the "earliest" analysis window that resulted in accurate transition detection, i.e., 500 ms, 400 ms, 300 ms or 200 ms, depending on during which analysis window the classification accuracy was highest.

G. Classifier Performance Evaluation

The performance of the various classifiers was evaluated in intra-subject analyses via leave-one-out cross validation with 10 trials collected from each subject. I.e., nine trials were used to train the classifier and the remaining trial was used to test/detect, then the process was iterated through all trials. All transitions were extracted based on foot switch signals and confirmed with video recordings. The classification

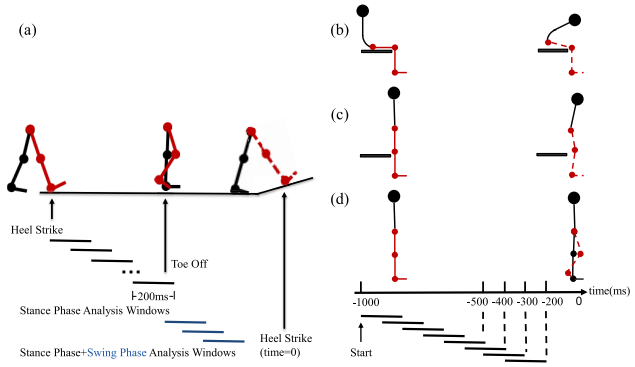

Fig. 5. Analysis windows illustration. The limb in focus is shown in red. Solid lines indicate the limb positions prior to the transition, and dashed lines indicate the limb positions at the instant of transition into the next mode. Analysis windows in the (a) dynamic states (there was an average of 7 analysis windows during stance analyse); (b) sit-to-stand transition; (c) stand-to-sit transition; and (d) standing still to level ground walking transition.

accuracy (CA) was defined as the total correct classified transitions divided by the total classified transitions, as a percent. The classification accuracy of the six states was computed and presented separately. The overall classification accuracy for each state was computed as the average of all subjects' classification accuracy. For each subject's data set, we repeated leave-one-out cross validation 15 times with between 1 and 15 muscle synergies, to determine the optimal number of muscle synergies. The number of sensors in the configuration that led to the best prediction accuracy was optimized by selecting the most important sensors among them.

Two-way repeated ANOVA analyses were used to compare CA among the different analysis windows and among the different sensor configurations. Post hoc paired t-tests were used to determine whether differences were observed between specific sensor configurations. Statistical significance was determined at the $p < 0.05$ level.

III. Results

For all states, transitions were generally predicted more accurately and earlier using extracted features from sensor configurations with IMU data than from only EMG data ($p < 0.05$). For all configurations and for all of the five dynamic states, transitions were predicted with higher CA when based on feature extraction from both the St+Sw analysis windows vs. only the St analysis windows ($p < 0.05$, Fig. 6). For all states, transitions predicted with sensor configurations 2-5, with a fusion of EMG (Ipsi or Bi) with Bi Acc and/or Gyr, and sensor configurations 6 and 7, with only mechanical sensor data, had higher CA than those predicted from sensor configuration 1 with only Ipsi EMG data ($p < 0.05$). For all six states, CA based on configurations 4 and 5 with Gyr data had less variance than that from configurations 1, 2, and 3 ($p < 0.05$), but not significantly less than that from configurations 6 and 7. For the five dynamic states, CA based on St+Sw analysis windows had less variance than the St analysis windows ($p = 0.026$).

In the walking state, all transitions could be well predicted based on sensor data from the St and the first two Sw

TABLE I
AVERAGE ± 1 STANDARD DEVIATION PREDICTION TIME OF THE TRANSITIONS FROM THE WALKING STATE

Transitions	Detected time of transitions prior to HS (ms)
W→W	388 ± 171
W→RA	394 ± 108
W→SD	394 ± 157
W→SA	281 ± 131
W→RD	356 ± 118
W→O	444 ± 105
W→FW	436 ± 160
W→ST	431 ± 103

TABLE II
CONFUSION MATRICES OF AVERAGE CLASSIFICATION ACCURACIES OF THE TRANSITIONS INCLUDED IN THE WALKING STATE

Pred / True	W→W	W→RA	W→SD	W→SA	W→RD	W→O	W→FW	W→ST
W→W	**91.3**	3.8	0	1.3	0	0	0	3.8
W→RA	1.3	**92.5**	2.5	2.5	1.3	0	0	0
W→SD	0	0	**95.0**	1.3	2.5	0	0	1.3
W→SA	1.3	8.8	0	**90.0**	0	0	0	0
W→RD	2.5	1.3	1.3	0	**92.5**	2.5	0	0
W→O	0	0	0	0	0	**98.8**	1.3	0
W→FW	0	1.3	0	1.3	2.5	0	**95.0**	0
W→ST	2.5	1.3	0	0	0	0	0	**96.3**

analysis windows (Table I). Transitions of W→O, W→FW, and W→ST were predicted with highest CA during the stance phase, and the other transitions except W→SA were predicted with highest CA using even the first Sw analysis window. All transitions were identified with CA≥90% (Table II). Using St+Sw analysis windows, highest CA of 95.1% ± 3.9% (mean ± 1 standard deviation) was found based on data from sensor configuration 5, followed by configuration 6, configuration 7, configuration 4, configuration 3, configuration 2 and finally configuration 1 (Fig. 6(a)). CA from configuration 5 was higher than that from configuration 6 ($p = 0.003$), and CA from configuration 4 was higher than that from configuration 7 ($p = 0.014$). Using the St analysis windows only, CA was highest at 85.2% ± 8.2% using sensor configuration 4, similar to configurations 3 and 5 with EMG and mechanical sensors and configurations 6 and 7 with only mechanical sensors. Higher CA was predicted from sensor configurations 3-7 than from configurations 1 and 2 ($p < 0.023$), among which CA from configuration 2 was higher than CA from configuration 1 ($p = 0.002$). CA from sensor configurations 6 and 7 were similar ($p = 0.510$).

In the static state, CA was higher using analysis windows including those 200-400 ms prior to the movement initiation than using analysis windows 500 ms prior to the movement initiation ($p < 0.05$), and based on fused EMG and IMU sensor data (Fig. 6(b)). Even so, the intentions to transition into Sit→ST, ST→Sit and ST→W based on sensor configurations 4 and 5 with EMG and Gyr data were predicted 500 ms prior to movement initiation with CA of 94.8% ± 3.3% and 95.2% ± 2.6%. CA from configuration 5 was higher than that from configuration 3 ($p = 0.049$), but not higher than that from configuration 4 ($p = 0.476$). CA from configuration 4 was not significantly higher than that from configuration 3 ($p = 0.076$) or configuration 7 ($p = 0.111$). CA from configuration 5 was not significantly higher than that from configuration 6 ($p = 0.097$).

In the RA state, classification using configuration 4 identified the transitions of RA→RA and RA→W in the 1-mode analysis with CA of 91.7% during the prior stance phase with a prediction time of 425 ± 52.5 ms, and in the 3-modes analysis with CA of 92.3% at 225 ± 141 ms prior to heel-strike. CA was highest based on sensor configuration 4, and once again using analysis windows in the St+Sw phases, in both the 3-modes classification and the 1-mode classification (Fig. 6(c)). CA was higher in the 1-mode classification than in the 3-modes classification in all seven sensor configurations using St ($p = 0.013$) and St+Sw ($p = 0.011$) analysis windows.

In the 3-modes classification using the St+Sw analysis, CA from configurations 4 and 5 were higher than those from configurations 6 and 7 ($p < 0.02$). In the 3-modes classification, RA_3→RA_3 and RA_3→W were identified with the highest CA, and RA_2→RA_2 and RA_2→W with the lowest (Table III).

In the RD state, classification using configuration 4 identified the transitions of RD→RD and RD→W in the 1-mode analysis with CA of 92.5% during the prior stance phase with a prediction time of 393.8 ± 49.6 ms. Transitions were identified with CA of 90.7% at 250 ms ± 71 ms prior to heel strike using configuration 5 in the 3-modes classification. Among the sensor configurations CA was again highest based on sensor configurations 4 and 5 (Fig. 6(d)). Using data in both the prior St and St+Sw analysis windows, CA was higher in the 1-mode classification than in the 3-modes classification ($p = 0.007$ and $p = 0.002$). CA from configurations 3-7 were higher than from configurations 1 and 2 ($p \leq 0.05$). CA from configuration 5 was higher than that from configuration 7 ($p = 0.027$), but not different than those from configurations 3 ($p = 0.103$), 4 ($p = 0.553$), and 6 ($p = 0.569$). CA from configuration 4 was higher that that from configuration 7 ($p = 0.019$), but was not significantly higher than from configuration 3 ($p = 0.088$). In the 3-modes classification, among the six transitions, RD_3→RD_3 and RD_3→W were identified with the highest CA (Table IV).

In the SA and SD states, the transitions of SA→SA, SA→W, SD→SD, and SD→W were identified with an average CA of 95.0% using St and one Sw analysis window. Among the sensor configurations, CA in the SA state was highest based on sensor configurations 4 and 5. CA in the SD state was highest based on sensor configurations 4, 5, and 7 (Fig. 6(e-f)). In both SA and SD state, CA from configuration 5 was higher than those from configurations 1 and 2 ($p < 0.05$), but not significantly higher than those from configurations 3-7. CA from configuration 4 was higher than that from configuration 1 ($p = 0.005$) but not significantly higher than that from configuration 2 ($p = 0.059$). In SD state, CA from configurations 4 were higher than that from configurations 1 and 2 ($p < 0.05$).

The classification accuracy was also affected by the number and the types of the extracted features. After preliminary

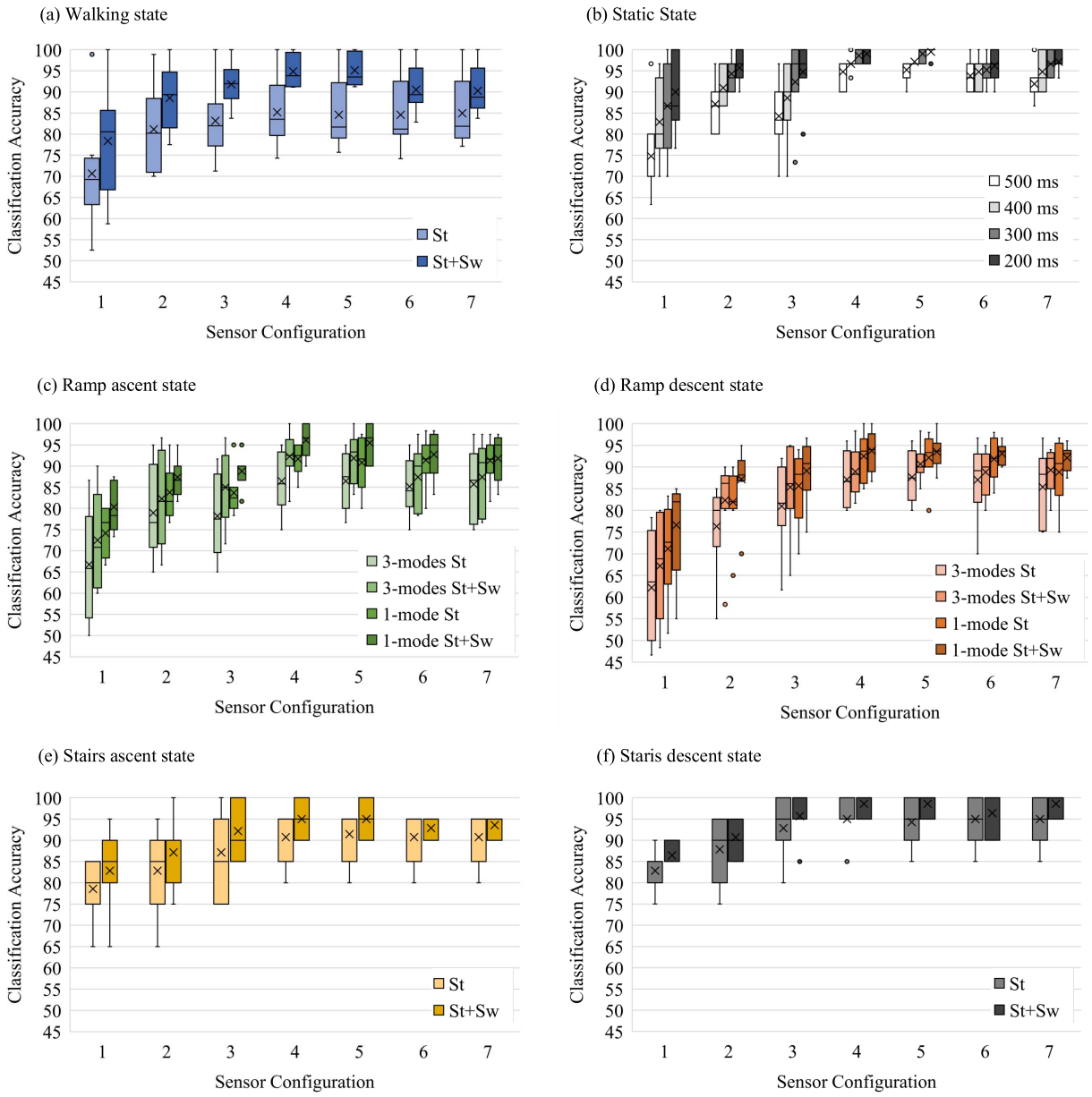

Fig. 6. Box plots of the classification accuracy with the 7 sensor configurations in the following states: (a) Walking state with the stance and stance + swing analysis windows; (b) Static state, with 4 analysis windows prior to movement; (c) Ramp ascent state with six and two modes, during stance and stance + swing analysis windows; (d) Ramp descent state with six and two modes, during stance and stance + swing analysis windows; (e) Stair ascending state during stance and stance + swing analysis windows; (f) Stair descending state during stance and stance + swing analysis windows. In all box plots, the line inside boxes represents median, the 'x' represents mean, the boxes represent the 1st and 3rd quartiles, the whiskers extend to the minimum and maximum values, and dots outside the whiskers represent outliers. Sensor configurations refer to 1) Ipsilateral EMG, 2) Bilateral EMG, 3) Ipsilateral EMG + Bilateral Acc, 4) Ipsilateral EMG + Bilateral Gyr, 5) Ipsilateral EMG + Bilateral Acc + Bilateral Gyr, 6) Bilateral Acc + Bilateral Gyr, and 7) Bilateral Gyr respectively.

testing with many combinations, the combination of four features from EMG data (mean absolute value, zero crossing, variance, and wave length) and six features from mechanical sensors data (mean absolute value, zero crossing, variance, wave length, slop sign changes, root mean square) presented the highest average classification accuracy. The optimal number of muscle synergies in the classifier varied among subjects, configurations and states. The optimal numbers of muscle synergies with configurations 5 were determined to be between 6-14 in the walking state and between 4-12 in the other five states. The optimal numbers of muscle synergies in the classifier tended to be larger for configurations with fused EMG and IMU data than for those with only EMG data. In configuration 5, CA was computed using all 11 EMG sensors, and again using the 6 most influential for each subject. Using 6 EMGs, in the walking state, an average CA of 84.7% was then achieved from St analysis windows, and 94.7% from St+Sw analysis windows, which were similar to those with configuration 5 including all 11 EMG signals ($p = 0.876$ and $p = 0.493$ respectively).

IV. Discussion

In this study, we enhanced the performance of a muscle synergy method to detect and classify intended motion by

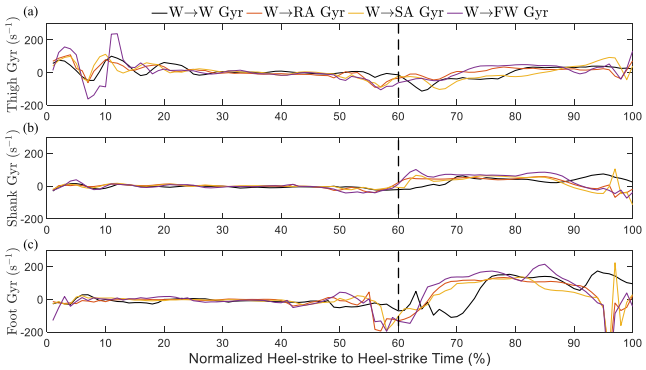

Fig. 7. Examples of angular velocity (Gyr) data in the heel-strike to heel-strike cycle prior to W→W, W→RA, W→SA and W→FW transitions in one subject. (a) Gyr data of the ipsilateral thigh segment; (b) Gyr data of the ipsilateral shank segment; (c) Gyr data of the ipsilateral foot segment. W: level ground walking, RA: ramp ascent, SA: stairs ascent, FW: fast speed walking.

TABLE III
CONFUSION MATRICES OF AVERAGE CLASSIFICATION ACCURACIES OF THE TRANSITIONS INCLUDED IN THE RAMP ASCENT (RA) STATE

True \ Pred	$RA_1 \rightarrow RA_1$	$RA_1 \rightarrow W$	$RA_2 \rightarrow RA_2$	$RA_2 \rightarrow W$	$RA_3 \rightarrow RA_3$	$RA_3 \rightarrow W$
$RA_1 \rightarrow RA_1$	**93.8**	6.3	0	0	0	0
$RA_1 \rightarrow W$	2.5	**90.0**	1.3	5.0	0	1.3
$RA_2 \rightarrow RA_2$	1.3	1.3	**88.8**	5.0	3.8	0
$RA_2 \rightarrow W$	0	3.8	5.0	**88.8**	0	2.5
$RA_3 \rightarrow RA_3$	0	0	0	0	**98.8**	1.3
$RA_3 \rightarrow W$	0	0	0	3.8	3.8	**92.5**

fusing EMG data with IMU data, in particular Acc and Gyr data. Furthermore, we successfully detected the intention to transition to a faster walking speed, and identified ramp walking at different inclination angles without an extra slope estimator, which both represent significant novelty. CA was generally higher when more sensor data was added to the classifier, particularly when Gyr data was involved in classification. Compared to a classifier based only on EMG data, by including mechanical sensor data, the classifier was able to detect intended transitions from a static or walking state sooner; many transitions could be accurately predicted during the stance phase prior to the transition into a new step, or more than 500 ms prior to movement initiation from a static state.

Our findings that the classifier performed better with fused sensor data from both EMGs and IMUs than with only EMGs agrees with findings from Huang *et al.* [9]. We can attribute this to the fact that different sensors can capture different information from the extracted features. Some movements have similar muscle synergy patterns as other movements, and are thus difficult to distinguish with only EMG data. Such movements may, however, exhibit different features in Acc and Gyr data. For example, muscle synergy patterns were relatively similar in W→W, W→RA, and W→FW, whereas linear acceleration and angular velocity of the ipsilateral thigh segment during early stance in the prior step were larger and more variable in W→FW than in W→W (Fig. 7). Configurations with mechanical sensors identified the transition of W→FW with CA of 95% (Table II), compared to a CA of 71.3% from Configuration 1 with only ipsilateral EMG data.

TABLE IV
CONFUSION MATRICES OF AVERAGE CLASSIFICATION ACCURACIES OF THE TRANSITIONS INCLUDED IN THE RAMP DESCENT (RD) STATE

True \ Pred	$RD_1 \rightarrow RD_1$	$RD_1 \rightarrow W$	$RD_2 \rightarrow RD_2$	$RD_2 \rightarrow W$	$RD_3 \rightarrow RD_3$	$RD_3 \rightarrow W$
$RD_1 \rightarrow RD_1$	**92.5**	2.5	2.5	1.3	1.3	0
$RD_1 \rightarrow W$	5.0	**87.5**	5.0	1.3	1.3	0
$RD_2 \rightarrow RD_2$	1.3	1.3	**92.5**	5.0	0	0
$RD_2 \rightarrow W$	0	1.3	5.0	**91.3**	0	2.5
$RD_3 \rightarrow RA_3$	0	1.3	1.3	1.3	**95.0**	1.3
$RD_3 \rightarrow W$	0	1.3	0	3.8	2.5	**92.5**

Afzal *et al.* [10] presented CA of 85% and 77.9% for RA and RD respectively with a muscle synergy method of motion detection using only EMG data; 11.4% of RA and 17.9% of RD were incorrectly identified as level ground walking. Our findings that Configuration 1 with Ipsi EMG presented a low CA in identifying W→RA and W→RD agree with their results. The transitions W→RA and W→RD were frequently incorrectly identified as W→W and W→ST. The CA of W→RA and W→RD were significantly improved to 92.5% with Configuration 5 with Ipsi EMG + Acc + Gyr (Table II). Using the transition of W→RA as an example, during the last stance phase analysis window, the angular velocity of the ipsilateral shank segment was lower in W→RA than in W→W, and was more varied in W→RA than in W→W(Fig. 7). The CA of W→RA was thus improved with fused sensor data.

Our finding that variance in CA was lowest with configurations 4 and 5 with fused EMG data and mechanical sensor data agrees with Young *et al.* [5]. This can be attributed to the mechanical sensors are generally more consistent than EMG signals with those of other trials from the same movements. We also observed that variance in CA with configurations 4 and 5 was lower in St+Sw analysis windows than in only St analysis windows, which we attributed to more kinematic changes in the swing phase than in the stance phase (Fig. 7). While the mechanical sensors were valuable in both stance and swing analysis windows, they were apparently even more valuable in the swing phase.

Among the three ramp angles in RA and RD states, ramp walking with inclination angle A_3 was identified with the highest CA, and A_2, the lowest. This is likely because A_3 ramp walking has more unique kinematic features than the other ramp angles, and that A_1 may be difficult to distinguish from A_2 ramp walking or level walking. For example, in $RA_3 \rightarrow RA_3$, there was most likely greater knee flexion and hip flexion at the beginning of the prior gait cycle than in the lower ramp angles and level ground. These kinematic features were very likely distinguishable from A_3 the Gyr data. Likewise, EMG data were apparently also most distinguishable in the steepest of the ramp angles, as muscle activations have likely differed notably from the lower ramp angles.

Our findings that classification based on sensor configuration 2 with Bi EMG presented was more accurate than CA based on configuration 1 with only ipsilateral EMG in static states indicate that EMG data from both sides helped to better distinguish between Sit→ST and ST→W than only unilateral EMG. Sit→ST is a symmetric transition, in contrast

to ST→W, and the additional EMG data from the contralateral leg, i.e. the trailing leg in gait initiation, resulted in more accurate classification. We also observed that classifications based on sensor configurations with Gyr data during the 500 ms prior to movement initiation were more accurate than those based only on EMG data. The Gyr data may have captured pelvis kinematic changes that occurred earlier than the EMG signals on the lower limbs were detected, as an IMU sensor was placed on the pelvis segment.

It is generally desirable to achieve the best prediction with as few sensors as possible. Depending on the application, it may be more practical to predict movement intentions from mechanical sensors alone, as their placement is less complicated and requires no particular skin preparation. We found that configurations 6 and 7 with only mechanical sensor data presented CA above 90% for all states, which may well be accurate enough for application in exoskeleton control. It is, however, worth noting that CA from fused IMU and EMG data was in several cases higher than with IMU data alone. This was particularly the case when detecting transitions in the walking state and in the RA state with the 3-modes analysis. This trade-off with sensor feasibility should be considered in each context. Furthermore, when EMGs were used to predict movement transitions, we found similar accuracy with as few as 6 EMG sensors as with all 11.

Regarding prediction time, our findings that the configurations with fused sensor data detected the intended movements and transitions earlier than configurations using only EMG data agrees with Huang *et al.* [9]. Except for the W→SA transition, the intentions to transition from the walking state were detected during the prior stance phase, which likely allows time for, e.g., an exoskeleton controller to adapt in real-time to the next locomotion mode. Similarly, transition intentions RA→RA, RA→W, RD→RD and RD→W were also detected accurately during the prior stance phase. Even from a static state, accurate prediction of the next locomotion mode were made 500 ms prior to motion, for instance, prior to toe-off in gait initiation. With our method, transitions can be predicted earlier than Wentik *et al.* [34], who detected gait initiation intention 130-260 ms prior to toe-off. Huang *et al.* [9] reported similar prediction times of RD→W as in the present study when they used the fused sensor data with EMG and ground reaction force data. As per the execution time, for both St and St+Sw analysis, after the last unit analysis window extracts features, it took less than 1.5 ms to identify the coming transition using a 16-core WIN computer. Using configuration 5 with the most sensor data, the execution time for a unit analysis window to extract features was less than 9.5 ms. Thus, the execution time of identifying a transition was always less than 10.5 ms, indicting our algorithm is compatible to real-time use.

The transitions to and from SA were accurately detected during the prior swing phase, and it is worth noting that these swing phases are longer those during level ground walking. Huang *et al.* stated that the intention of transition W→SA should be detected before toe-off to allow the knee to generate adequate flexion torque needed for climbing stairs. Our algorithm detected the intentions of W→SA accurately at 200 ms after toe-off. This may limit the use of this method in real-time. However, its performance needs to be further validated in real-time implementation, and the critical prediction time may depend on the assistive strategies.

The classifier in the walking state could not reliably distinguish the angle of the forthcoming ramp, neither whether transitioning into RA or RD. In the RA and RD states, however, the transitions among different inclination angles were predicted accurately during the prior swing phase, indicating that our method was able to identify and distinguish among locomotion modes with different inclination angles. Identifying ramp angle may be important as it may influence an exoskeleton's assistance strategy [30]. To the best of our knowledge, this is the first study presenting a method that can successfully identify ramp walking at different inclination angles without using a slope estimator. It is also, to the best of our knowledge, the first study presenting a method that can accurately identify the intention to change walking speed and to cease walking.

Huang *et al.* and Afzal *et al.* used the concept of echo control in their studies, in which the subjects were asked to perform transitions with the leading limb which was not instrumented with sensors, and the other limb's signals were used to identify the locomotion intentions [9], [10]. Varol *et al.* [29] used joint angles and angular velocities to identify different modes (sitting, standing, stairs climbing, and walking) using Gaussian mixture models. Parri *et al.* used joint angles to identify different modes (sitting, standing and walking) by setting thresholds of joint angles in each mode [26]. Their methods focused on identifying the current locomotion mode, instead of predicting the next locomotion mode. In contrast to these studies, we used wearable sensor data from the right limb's motion to predict the next step of the same limb, and can thus achieve a greater prediction time. Echo control may clearly be most useful in control of unilateral prostheses. However, in bilateral exoskeleton control, there may be no 'sound' limb to mimic. Our study thus presented a possibility to identify motion transition intentions without referring to a leading or a trailing limb.

One of the limitations with this study is that we only tested on able-bodied subjects who wore no exoskeletons, powered or unpowered, whereas it has been reported that powered exoskeletons will influence users' movement and muscle activations [35]. Our classifier should, however, be able to adapt to that situation. Further studies are warranted to develop this enhanced muscle synergy method to adapt to changes caused when donning a powered exoskeleton, and to implement the predictions in real-time. Studies on subjects with lower limb weakness or altered muscle tone should also be conducted, as their locomotion patterns and muscle activation patterns will differ from those of able-bodied subjects. The method presented in our study is, however, subject-specific; in patients who do not have normal muscle control, if fixed sensor signal patterns during movements and transitions can be identified, the classifier should also work for them, regardless of whether the patterns are similar to those from able-bodied people. If not, this method will not be suitable. For such a patient group in which this classifier may not work, incorporating a

wearable camera to recognize coming terrains may assist in achieving smooth transitions.

V. Conclusion

We have improved a muscle synergy method to detect movement intention by fusing EMG data with IMU data; methods using fused sensor data classified transitions between different locomotion modes and states with higher accuracy that those based solely on EMG data. Notably, our method was able to accurately identify and distinguish among transitions of ramp walking at different inclination angles, as well as transitions from one walking speed to another. Two static modes, seven dynamic modes, and the 27 transitions among them were identified with an overall average classification accuracy of 94.5%. Using this method, we were able to predict most transitions during the swing and even stance phase prior to the transition. For nearly all transitions, we were able to predict the next locomotion mode 300-500 ms prior to the step into that mode, sometimes even sooner, indicating promising application in exoskeleton control.

References

[1] S. R. Chang *et al.*, "A muscle-driven approach to restore stepping with an exoskeleton for individuals with paraplegia," *J. NeuroEng. Rehabil.*, vol. 14, no. 1, p. 48, Dec. 2017.

[2] S. Au, M. Berniker, and H. Herr, "Powered ankle-foot prosthesis to assist level-ground and stair-descent gaits," *Neural Netw.*, vol. 21, no. 4, pp. 654–666, May 2008.

[3] M. Sartori, D. G. Llyod, and D. Farina, "Neural data-driven musculoskeletal modeling for personalized neurorehabilitation technologies," *IEEE Trans. Biomed. Eng.*, vol. 63, no. 5, pp. 879–893, May 2016.

[4] O. Bai *et al.*, "Prediction of human voluntary movement before it occurs," *Clin. Neurophysiol.*, vol. 122, no. 2, pp. 364–372, Feb. 2011.

[5] A. J. Young, T. A. Kuiken, and L. J. Hargrove, "Analysis of using EMG and mechanical sensors to enhance intent recognition in powered lower limb prostheses," *J. Neural Eng.*, vol. 11, no. 5, Oct. 2014, Art. no. 056021.

[6] J. A. Spanias, E. J. Perreault, and L. J. Hargrove, "Detection of and compensation for EMG disturbances for powered lower limb prosthesis control," *IEEE Trans. Neural Syst. Rehabil. Eng.*, vol. 24, no. 2, pp. 226–234, Feb. 2016.

[7] H. Huang, T. A. Kuiken, and R. D. Lipschutz, "A strategy for identifying locomotion modes using surface electromyography," *IEEE Trans. Biomed. Eng.*, vol. 56, no. 1, pp. 65–73, Jan. 2009.

[8] M. Sartori, M. Reggiani, E. Pagello, and D. G. Lloyd, "Modeling the human knee for assistive technologies," *IEEE Trans. Biomed. Eng.*, vol. 59, no. 9, pp. 2642–2649, Sep. 2012.

[9] H. Huang, F. Zhang, L. J. Hargrove, Z. Dou, D. R. Rogers, and K. B. Englehart, "Continuous locomotion-mode identification for prosthetic legs based on neuromuscular–mechanical fusion," *IEEE Trans. Biomed. Eng.*, vol. 58, no. 10, pp. 2867–2875, Oct. 2011.

[10] T. Afzal, K. Iqbal, G. White, and A. B. Wright, "A method for locomotion mode identification using muscle synergies," *IEEE Trans. Neural Syst. Rehabil. Eng.*, vol. 25, no. 6, pp. 608–617, Jun. 2017.

[11] B. Kibushi, S. Hagio, T. Moritani, and M. Kouzaki, "Speed-dependent modulation of muscle activity based on muscle synergies during treadmill walking," *Frontiers Hum. Neurosci.*, vol. 12, p. 4, Jan. 2018.

[12] S. Hagio, M. Fukuda, and M. Kouzaki, "Identification of muscle synergies associated with gait transition in humans," *Frontiers Hum. Neurosci.*, vol. 9, p. 48, 2015.

[13] A. Saito, A. Tomita, R. Ando, K. Watanabe, and H. Akima, "Muscle synergies are consistent across level and uphill treadmill running," *Sci. Rep.*, vol. 8, no. 1, pp. 1–10, Dec. 2018.

[14] J. Esmaeili and A. Maleki, "Comparison of muscle synergies extracted from both legs during cycling at different mechanical conditions," *Australas. Phys. Eng. Sci. Med.*, vol. 42, no. 3, pp. 827–838, 2019.

[15] N. Bu, M. Okamoto, and T. Tsuji, "A hybrid motion classification approach for EMG-based human–robot interfaces using Bayesian and neural networks," *IEEE Trans. Robot.*, vol. 25, no. 3, pp. 502–511, Jun. 2009.

[16] R. C. King, E. Villeneuve, R. J. White, R. S. Sherratt, W. Holderbaum, and W. S. Harwin, "Application of data fusion techniques and technologies for wearable health monitoring," *Med. Eng. Phys.*, vol. 42, pp. 1–12, Apr. 2017.

[17] S. Kyeong, W. Shin, and J. Kim, "Predicting walking intentions using sEMG and mechanical sensors for various environment," in *Proc. 40th Annu. Int. Conf. IEEE Eng. Med. Biol. Soc. (EMBC)*, Jul. 2018, p. 4414.

[18] D.-H. Moon, D. Kim, and Y.-D. Hong, "Intention detection using physical sensors and electromyogram for a single leg knee exoskeleton," *Sensors*, vol. 19, no. 20, p. 4447, Oct. 2019.

[19] L. Du, F. Zhang, M. Liu, and H. Huang, "Toward design of an environment-aware adaptive locomotion-mode-recognition system," *IEEE Trans. Biomed. Eng.*, vol. 59, no. 10, pp. 2716–2725, Oct. 2012.

[20] T. Afzal, G. White, A. B. Wright, and K. Iqbal, "Locomotion mode identification for lower limbs using neuromuscular and joint kinematic signals," in *Proc. 36th Annu. Int. Conf. IEEE Eng. Med. Biol. Soc.*, Aug. 2014, pp. 4071–4074.

[21] K. Takahashi, M. Lewek, and G. Sawicki, "A neuromechanics-based powered ankle exoskeleton to assist walking post-stroke: A feasibility study," *J. Neuroeng. Rehabil.*, vol. 12, p. 15, Dec. 2015.

[22] D. Joshi and M. E. Hahn, "Terrain and direction classification of locomotion transitions using neuromuscular and mechanical input," *Ann. Biomed. Eng.*, vol. 44, no. 4, pp. 1275–1284, Apr. 2016.

[23] Q. Ai, Y. Zhang, W. Qi, Q. Liu, and A. K. Chen, "Research on lower limb motion recognition based on fusion of sEMG and accelerometer signals," *Symmetry*, vol. 9, no. 8, p. 147, Aug. 2017.

[24] W. Wang, B. Chen, P. Xia, J. Hu, and Y. Peng, "Sensor fusion for myoelectric control based on deep learning with recurrent convolutional neural networks," *Artif. Organs*, vol. 42, no. 9, pp. E272–E282, Sep. 2018.

[25] K. Tanghe, F. De Groote, D. Lefeber, J. De Schutter, and E. Aertbelien, "Gait trajectory and event prediction from state estimation for exoskeletons during gait," *IEEE Trans. Neural Syst. Rehabil. Eng.*, vol. 28, no. 1, pp. 211–220, Jan. 2020.

[26] A. Parri *et al.*, "Real-time hybrid locomotion mode recognition for lower limb wearable robots," *IEEE/ASME Trans. Mechatronics*, vol. 22, no. 6, pp. 2480–2491, Dec. 2017.

[27] X. Liu and Q. Wang, "Real-time locomotion mode recognition and assistive torque control for unilateral knee exoskeleton on different terrains," *IEEE/ASME Trans. Mechatronics*, vol. 25, no. 6, pp. 2722–2732, Dec. 2020.

[28] V. Ruiz Garate *et al.*, "Experimental validation of motor primitive-based control for leg exoskeletons during continuous multi-locomotion tasks," *Frontiers Neurorobot.*, vol. 11, p. 15, Mar. 2017.

[29] H. A. Varol, F. Sup, and M. Goldfarb, "Multiclass real-time intent recognition of a powered lower limb prosthesis," *IEEE Trans. Biomed. Eng.*, vol. 57, no. 3, pp. 542–551, Mar. 2010.

[30] F. Sup, H. A. Varol, and M. Goldfarb, "Upslope walking with a powered knee and ankle prosthesis: Initial results with an amputee subject," *IEEE Trans. Neural Syst. Rehabil. Eng.*, vol. 19, no. 1, pp. 71–78, Feb. 2011.

[31] H. J. Hermens *et al.*, "European recommendations for surface electromyography, results of the SENIAM project," Roessingh Res. Develop., Enschede, The Netherlands, 1999.

[32] S. A. Murray, K. H. Ha, C. Hartigan, and M. Goldfarb, "An assistive control approach for a lower-limb exoskeleton to facilitate recovery of walking following stroke," *IEEE Trans. Neural Syst. Rehabil. Eng.*, vol. 23, no. 3, pp. 441–449, May 2015.

[33] K. Yuan *et al.*, "A realtime locomotion mode recognition method for an active pelvis orthosis," in *Proc. IEEE/RSJ Int. Conf. Intell. Robots Syst. (IROS)*, Sep. 2015, pp. 6196–6201.

[34] E. C. Wentink, S. I. Beijen, H. J. Hermens, J. S. Rietman, and P. H. Veltink, "Intention detection of gait initiation using EMG and kinematic data," *Gait Posture*, vol. 37, no. 2, pp. 223–228, Feb. 2013.

[35] K. M. Steele, R. W. Jackson, B. R. Shuman, and S. H. Collins, "Muscle recruitment and coordination with an ankle exoskeleton," *J. Biomech.*, vol. 59, pp. 50–58, Jul. 2017.